2 September 2002

PHYSICS LETTERS A

ELSEVIER

Physics Letters A 301 (2002) 451–461

www.elsevier.com/locate/pla

Global quantum Hall phase diagram from visibility diagrams

F. Chandelier [a], Y. Georgelin [a], T. Masson [b,∗], J.-C. Wallet [a]

[a] *Groupe de Physique Théorique, Institut de Physique Nucléaire, F-91406 Orsay Cedex, France*
[b] *Laboratoire de Physique Théorique (UMR 8627), Bât 210, Université Paris-Sud Orsay, F-91405 Orsay Cedex, France*

Received 17 May 2002; accepted 24 July 2002

Communicated by J. Flouquet

Abstract

Starting from a framework encoding rather simple symmetry principle based on modular subgroups, we construct a zero temperature global phase diagram for the QHE. This phase diagram is found to involve two insulating phases. One noticeable prediction is the possibility to have direct transitions from an insulting phase to any integer ν as well as $\nu = 1/(2k+1)$ ($k \in \mathbb{N}$) fractional quantum Hall liquid phases which seems to agree with some recent experimental observations. We also propose selection rules for the possible plateau–plateau (and plateau–insulator) transitions which may constitute testable predictions.

1. Introduction

A two-dimensional electron gas submitted to a perpendicular magnetic field exhibits a large variety of interesting behaviours, among which the Quantum Hall Effect (QHE) appearing to be a fascinating phenomenon [1]. This has been subject of intense theoretical and experimental investigations aiming to get a more complete understanding of the hierarchical structure of the Hall plateaus, the properties and the very nature of the transitions observed among plateaus together with a complete characterization of the corresponding phase diagram [2].

Many attempts have been invested in a formulation of an effective theory capturing the essential low energy features of the (integer as well as fractional) quantum Hall liquid states. First progress in this direction has been carried out in [3] and further developed in [4] from which by further introducing phenomenological considerations, a theoretical phase diagram for the QHE has been proposed [5]. It has been realized for some time that modular symmetries [6] may be helpful tools to describe some global features of the QHE, in the lack of a fully satisfactory (effective or microscopic) theory for the QHE. Earliest works in this direction [7] have considered some possible candidates as modular symmetries relevant to the QHE, some of which being ruled out from phenomenological analysis. Two subgroups of the modular groups have finally appeared to be appealing candidates. They are known in the mathematical literature respectively,

∗ Corresponding author.
E-mail address: thierry.masson@th.u-psud.fr (T. Masson).

0375-9601/02/$ – see front matter
PII: S0375-9601(02)01051-4

as $\Gamma_0(2)$ (underlying the "law of the corresponding states" introduced in [5] as shown, e.g., in [8]) and $\Gamma(2)$ (a subgroup of $\Gamma_0(2)$) and their physical implications for the QHE have been studied in detail respectively in [9] and [10a–c].

In [10b], important building blocks connected to those modular subgroups, called visibility diagrams, have been introduced and described and further exploited in [10c]. They appear to encode a great amount of information on the physics of the quantum Hall systems which can be extracted through the introduction of a natural mapping between those diagrams and the relevant physical quantities. Such a mapping has been used in [10b] to derive from the visibility diagrams a resistivity plot which fits well with the experimental data. In the same way in [10c], it has been shown that the stripe structure which appears in those visibility diagrams reproduces nicely the experimentally observed stripe structure occurring in the gate voltage-magnetic field plane which has been evidenced in a recent experiment [11] on the conductance fluctuations in the (integer) quantum Hall regime. These observations seem to indicate that the visibility diagrams encode interesting physical features of the QHE and motivate us to extend the phenomenological lines introduced in [10b,10c] to a phenomenological construction of a zero temperature global phase diagram for the QHE and to confront the corresponding predictions to the experimental observations. This is the purpose of the present Letter.

We find in particular that the topology of the phase diagram we obtain is in good agreement with (some of) the experimental observations that have been reported [12]. To be self-contained, we recall in Section 2 the essential features of the visibility diagrams and of the corresponding modular subgroups. The construction of the global phase diagram is presented in Section 3. One of the salient features of this phase diagram which appears to involve two insulating phases, is that it predicts the occurrence of allowed direct transitions from some insulator to any integer ν as well as $\nu = 1/(2k+1)$ ($k \in \mathbb{N}$) fractional quantum Hall liquid phases which seems to agree with some recent experimental observations [12]. This is analyzed and discussed in Section 4, where we also propose selection rules for the possible plateau–plateau (and plateau–insulators) transitions that we confront to the one derived in [5].

2. The visibility diagrams

2.1. Basic features

In what follows, we collect the essential features of the visibility diagrams which are connected to $\Gamma(2)$ and that will be needed in the analysis. First, recall that the subgroup $\Gamma(2)$ of the modular group $\Gamma(1)$ [6] is the set of transformations acting on $\mathbb{P}^* = \mathbb{P} \cup \mathbb{Q}$ defined by[1]

$$G(z) = \frac{uz+v}{tz+w}, \quad u, v, t, w \in \mathbb{Z}, (u, v) \text{ odd}, \ (t, w) \text{ even} \tag{1a}$$

$$uw - tv = 1 \text{ (unimodularity condition)} \tag{1b}$$

and is generated by

$$T^2(z) = z + 2, \tag{2a}$$

$$\Sigma(z) = ST^{-2}S(z) = \frac{z}{2z+1} \tag{2b}$$

where $T(z) = z + 1$ and $S(z) = -1/z$ are the generators of $\Gamma(1)$, while the complex coordinate is identified in physical applications with the complex conductivity. Namely, one has $z = \sigma_H + i\sigma_L$ where σ_H (respectively, σ_L) is the Hall (respectively, longitudinal) conductivity.

From this modular subgroup $\Gamma(2)$ one can construct a model for the classification of the integer and fractional Hall states [10b] by restricting $\Gamma(2)$ to act only on the real part of the complex conductivity identified with the filling factor ν (parametrized as $\nu = p/q \in \mathbb{Q}$). This model[2] reproduces successfully the observed hierarchical structures of the Hall states as shown in [10b] (see also first of [10a]). Furthermore, one can show that the constraints stemming from $\Gamma(2)$ on a physically admissible family of β-functions permit one to reproduce (most of) the present experimental observations and in particular give rise, upon integration of the β-functions, to a shape of the crossover

[1] $\mathbb{P}$ is the open upper complex plane with complex coordinate z ($\Im z > 0$) and $\mathbb{Q}$ is the set of rational numbers.

[2] The model refines the Jain classification and involves a modification of the law of the corresponding states proposed in [5]. This latter law is based on the modular subgroup $\Gamma_0(2)$ involving $\Gamma(2)$ as a subgroup.

for the various transitions in good (qualitative) agreement with the experimental observations (see second of Ref. [10a]).

In addition to the action of $\Gamma(2)$ itself, the above constructions involve other important building blocks. These latter are called visibility diagrams and have been introduced and described in some detail in [10b] and further exploited in [10c]. They appear to encode a great amount of information on the physics of the quantum Hall systems which can be extracted through the introduction of a natural mapping between those diagrams and the relevant physical quantities (combined with a consistent physical interpretation of the generators of $\Gamma(2)$). Such a mapping has been used in [10b] to derive from the visibility diagrams a resistivity plot which fits very well with the experimental data. In the same way in [10c], it has been shown that the stripe structure which necessarily appears in those visibility diagrams reproduces nicely the experimentally observed stripe structure occurring in the gate voltage-magnetic field plane which has been evidenced in a recent experiment on the conductance fluctuations in the quantum Hall regime and reported in [11]. The construction of the visibility diagrams is now recalled.

Basically, the visibility diagrams can be viewed as simple pictorial devices for the construction of Farey sequences [6] of rational numbers p/q, where p and q are relatively prime positive (or zero) integers. They can be presented on two-dimensional square lattices in which any rational number p/q is represented by a vertex with coordinate (q, p). In the following, it will be convenient to consider successively 3 possible types of pairs (q, p), namely pairs with q odd and p odd, q odd (respectively, even) and p even (respectively, odd). These 3 types of pairs will give rise to the 3 different visibility diagrams which are involved in our analysis.

Now, there is a well-known theorem in arithmetics stating that for any relatively prime integers q and p, there exist two set of pairs (a, b) and (a', b') where a and b and a' and b' are necessarily relatively prime integers satisfying

$$qb - pa = +1, \tag{3a}$$

$$qb' - pa' = -1. \tag{3b}$$

Then, applying first the above mentioned theorem to the pairs (q odd, p odd) leads therefore to the introduction of all possible pairs (a, b) (respectively, (a', b')) satisfying (3a) (respectively, (3b))[3] which can be displayed on a two-dimensional lattice as shown on Fig. 1. Those pairs are aligned on two half straight lines on this lattice which define a stripe (surrounding only the pair (q, p)). The resulting visibility diagram, called odd–odd diagram, is then obtained by drawing on the lattice the stripes associated to all possible pairs (q odd, p odd), as depicted on Fig. 1. A similar procedure applied to the pairs (q odd, p even) (respectively, (q even, p odd)) leads to the even–odd (respectively, odd–even) diagram depicted on Fig. 2 (respectively, Fig. 3). Notice that in those diagrams, each stripe is completely characterized by a pair (q, p) or equivalently by its slope p/q so that each stripe will be indexed by p/q. Then, according to [10b], any stripe for which q is odd (respectively, even) is identified with

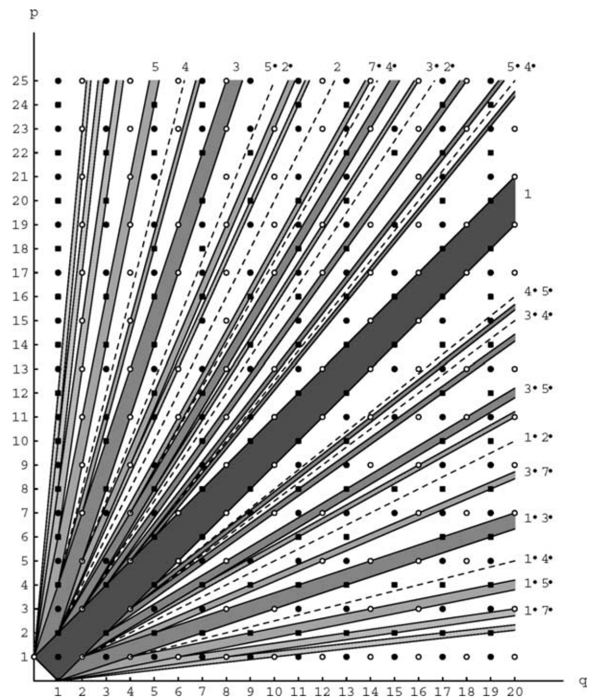

Fig. 1. The odd–odd visibility diagram. Each stripe is represented as a dark area, indexed by its respective filling factor which is also equal to the slope of that stripe. Circle (respectively, square) points on this diagram correspond to p odd (respectively, even) and black (respectively, white) points correspond to q odd (respectively, even).

[3] One can easily realize that all the pairs (a, b) and (a', b') can never be of (odd, odd) type.

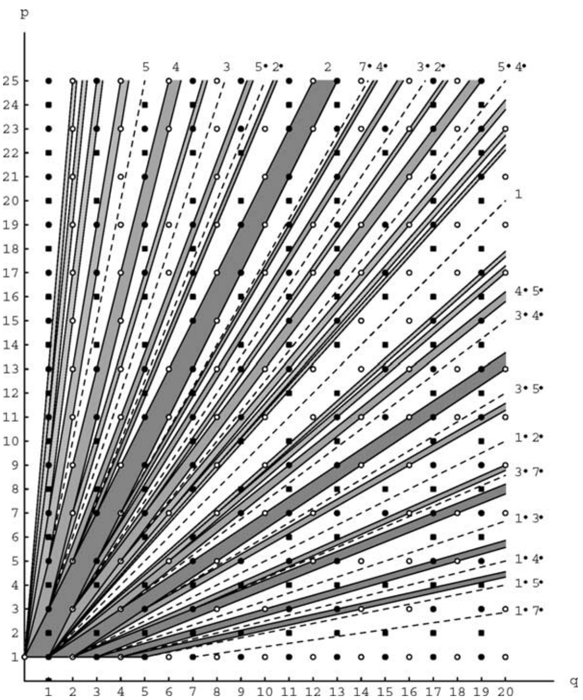

Fig. 2. The odd–even visibility diagram with stripes represented as in Fig. 1.

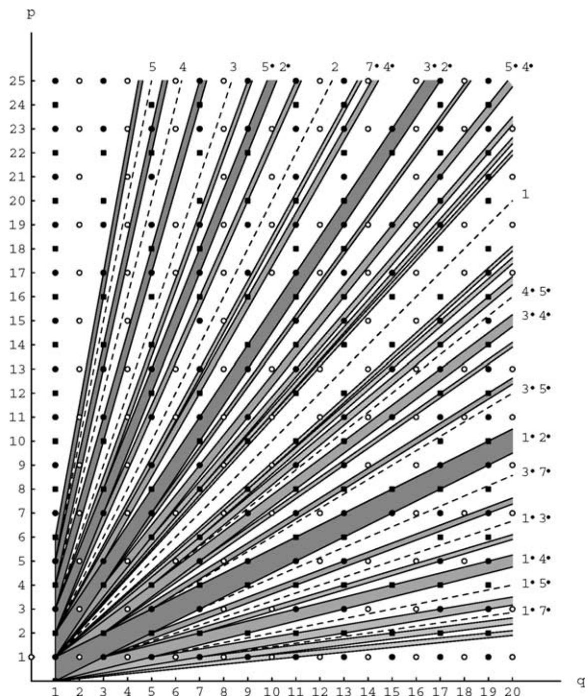

Fig. 3. The even–odd visibility diagram. The conventions are similar to those for Fig. 1.

a quantum Hall liquid state, that is a plateau, (respectively, "metallic" Hall state) with corresponding filling factor $p/q = \nu$.

To close this subsection, we recall that the even–odd and odd–odd diagrams corresponds to quantum Hall liquid phases indexed by filling factors respectively with even and odd numerators. This reflects the fact that the action of $\Gamma(2)$ on rational numbers preserves the even or odd character of the numerators as it can be seen for instance from the very definition of $\Gamma(2)$ given in (1a). We mention by the way that there have been some experimental indications that even and odd numerator states may well behave differently [13]. Besides, it can be realized that the even–odd diagram supplemented by the diagram obtained from the superposition of the odd–even and odd–odd diagrams is naturally related to the modular subgroup $\Gamma_0(2)$ (which treats even and odd numerator states on an equal footing). This latter subgroup of the modular group is generated by $T(z)$ and $\Sigma(z)$, involves $\Gamma(2)$ as a subgroup and is the symmetry underlying the law of the corresponding states proposed in [5]. The respective physical implication of $\Gamma(2)$ and $\Gamma_0(2)$ will be discussed in Section 4. For the construction of a global phase diagram for the QHE, it appears that treating separately even and odd numerator filling factor states proves useful. This amounts to consider the three visibility diagrams mentioned above. In particular, this allows one to deal conveniently with the possible occurrence of overlaps of stripes considered in Section 3.

2.2. The physical mapping

As already mentioned above, the visibility diagrams encode a great amount of physical information on the quantum Hall systems which can be extracted when a natural mapping between the diagrams and the relevant physical quantities is introduced. This mapping allows one to built a consistent physical interpretation of the visibility diagrams and is based essentially on the very definition of the filling factor ν in term of the number of charge carrier and number of unit flux combined with a physical interpretation of the generators of $\Gamma(2)$, as we now recall for sake of completeness. One first observe that the filling factor

ν is defined by

$$\nu = \frac{N_c}{N_\phi}, \tag{4}$$

where N_c (respectively, N_ϕ) denotes the number of charge carriers (respectively, the number of unit flux). One further observes that ν is identified with p/q in the visibility diagrams and that N_ϕ is related to the applied magnetic field B through $N_\phi = BSh/e$ (S is the device area) while N_c, the number of charge carriers is essentially controlled by the applied gate voltage V_g. Bringing this together, this suggests identifying the (q, p) plane of the visibility diagrams with the (N_ϕ, N_c) plane or alternatively with the (B, V_g) plane through the mapping

$$q \mapsto N_\phi \quad \text{or} \quad q \mapsto B, \tag{5a}$$

$$p \mapsto N_c \quad \text{or} \quad p \mapsto V_g. \tag{5b}$$

It can be realized that (5) is consistent with the action of $\Gamma(2)$ on the vertices of the diagrams as shown in [10c]. Indeed, the action of the operator T^2 on any vertex (q, p) produces a vertical shift given by $(q, p) \mapsto (q, p + 2q)$. Physically, T^2 is a Landau shift type operator acting on the filling factor as $\nu \mapsto \nu + 2$ and corresponds to an increase of the number of charge carriers which is consistent with (5b). On the other hand, the action of the operator Σ, interpreted as the flux attachment operator corresponding to an increase of the applied magnetic field B (or N_ϕ), on any vertex (q, p) produces a horizontal shift given by $(q, p) \mapsto (q + 2p, p)$ which is therefore consistent with (5a). Note that the above discussion can be reproduced for $\Gamma_0(2)$, with T^2 replaced by T, the usual Landau level addition operator, showing that (5) is consistent with the action of $\Gamma_0(2)$ as well.

Concerning the operator $T^2(z)$, one comment is in order. Consider first the operator $T(z)$ associated with the Landau level addition symmetry. The physical assumption underlying this symmetry is that the physics at any partially filled Landau level does not depend of the number of completely filled lower Landau levels. This assumption is quite plausible for well separated Landau levels but seems more questionable if any two Landau levels become close to each other which can be produced when a Zeeman-type splitting comes into play. Basically, if the value of the ratio of the Zeeman energy to the cyclotron energy is small (or around one half), the splitted Landau levels come to be organized into well separated pairs, each level being close to each other within each pair. In that limiting situation, the physics of the upper level of a pair may well be influenced by the electrons located in the lower level of that pair while it seems still relevant to assume that the physics of any pair is independent of the number of how much pairs below are filled. A possible way to take this into account is to replace $T(z)$ by the operator $T^2(z)$ (see third of Ref. [9]). Whether this replacement can be still reasonably performed or not for other values of the Zeeman to cyclotron energy ratio depends in fact on the new organization of the splitted Landau levels. For instance, if for some reasons in an experiment the Zeeman to cyclotron energy ratio would be close to 1, the splitted levels would be evenly spaced with spacing close to the cyclotron energy, so that Landau level addition would more likely correspond to $T(z)$. We will come back to this point when we compare the predictions stemming from the global phase diagram we propose to some experimental observations in Section 4.

In [10b], we combined (5) with visibility diagrams to obtain a successful description of the observed architecture of the quantum Hall states and to derive a (zero temperature) resistivity plot fitting very well with the experimental data. In the same way in [10c], we have shown that the stripe structure appearing in the visibility diagrams reproduces nicely the experimentally observed stripe structure occurring in the (B, V_g) plane which has been recently reported in [11]. Keeping these results in mind, it seems reasonable to extend the lines of analysis presented in [10b, 10c] to construct from the visibility diagrams a zero temperature global phase diagram for the QHE. The corresponding construction is now described.

3. Construction of the global phase diagram

Owing to the discussion presented in Section 2.2 and the mapping (5), we identify from now on the p (respectively, q) axis of the visibility diagrams with N_c (respectively, $N_\phi \sim B$). Now, consider first the case of quantum Hall liquid phases which in the present framework are identified with the odd denominator stripes involved in the even–odd and odd–odd diagrams (the case of the even denominator stripes corresponding to "metallic" states will be examined later on).

Among various possible representations of a zero temperature phase diagram for the QHE, we choose two which, we think, permit one to compare easily the predictions stemming from the present framework to experimental results. Namely, we choose to represent the phase diagram in the (B, N_c) plane and in the $(1/\nu,\ N_c)$ plane. From the discussion of Section 2.2, the (B, N_c) plane is directly linked with the plane of the visibility diagrams through (5) while the $(1/\nu,\ N_c)$ plane is connected to the (q, p) plane by making use of (4) and (5). Choosing those planes permits us to compare directly our phase diagram with the experimental data in [12]. Keeping this in mind, the obtention of the topology of the phase diagram (in the (B, N_c) plane) for the quantum liquid states counterpart follows from the superposition of the two above mentioned visibility diagrams, up to the possible occurrence of overlaps between some stripes in these diagrams. This last point is now examined and confronted to some experimental features of the QHE from which we will define a simple prescription to deal with the possible overlaps of some stripes.

To see that, recall that in the present framework, the q (respectively, p) axis is identified with B (respectively, N_c). Let us first assume that N_c is fixed to a given value, says $N_c = N_0$. Then, when B increases, one moves on the diagrams on a horizontal line defined by $N_c = N_0$. Now, for this value of N_c, the plateaus are not all experimentally accessible. This corresponds in the present scheme to the fact that these nonobservable plateaus and therefore their corresponding odd denominator stripes are associated with (rational) values of $\nu = p_1/q_1$ such that $p_1 > N_0$. These plateaus would become experimentally observable for a larger value of N_c. Accordingly, the domain corresponding to an experimentally accessible stable phase $\nu = p_1/q_1$ of the QHE must be in the upper half plane $N_c > N_0$. A similar analysis at fixed $B = B_0$ can be performed to restrict the domain of experimentally accessible stable phase $\nu = p_1/q_1$ to the right half plane $q_1 > B_0$.

Now, the above observation (and further noticing that two odd denominator stripes can overlap only near their indexing vertices) suggests a simple way to modify slightly the boundaries of the overlapping stripes leading to nonoverlapping phase domains. Indeed, one assumes that the (q, p) vertex indexing an odd denominator stripe is the lower left wedge of the corresponding phase domain in the phase diagram. In that way, the new boundary of an odd denominator stripe that will give rise to a phase domain in the phase diagram joins the indexing vertex (q, p) of that stripe to the nearest point (a, b) on the boundary of the stripe with $a \geqslant q$, $b \geqslant p$.

Applying the above prescription to the odd–odd and odd–even visibility diagrams yields to a prediction for a zero temperature phase diagram for the QHE, depicted in the (B, N_c) plane on Fig. 4 and in the $(1/\nu,\ N_c)$ plane on Fig. 5. Notice that by choosing the $(1/\nu,\ 1/N_c)$ plane, this phase diagram shows a more compact aspect, where many more phases can be represented (Fig. 6). This last diagram will not be used in the forthcoming analysis. The symmetries of the diagram depicted on Fig. 4 are the same as the one for

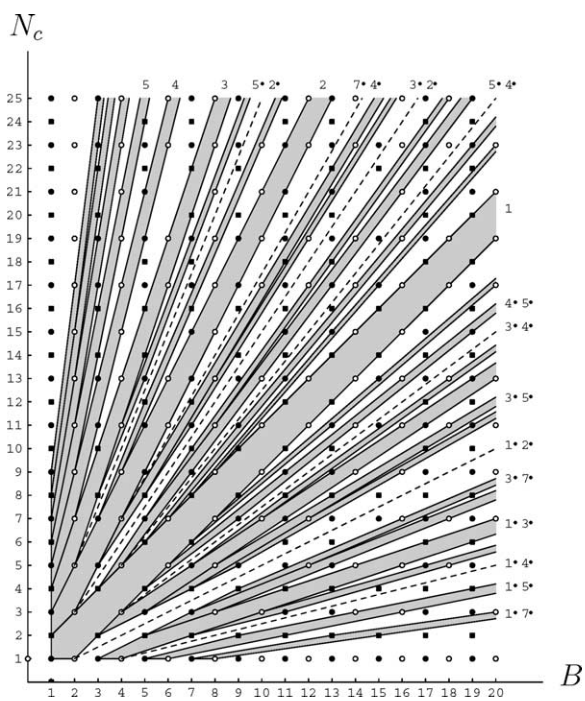

Fig. 4. Zero temperature global phase diagram in the (B, N_c) plane. The domains corresponding to expected stable quantum Hall liquid phases are depicted as dark areas, each one being labelled by its corresponding filling factor. Note the occurrence of the 2 white regions along the N_c and B axis, corresponding respectively to $\nu =$"1/0" (insulator Ins_V, vertical stripe) and $\nu = 0/1$ (insulator Ins_H, horizontal stripe). The dashed lines represent some metallic states corresponding to the directions of the stripes in Fig. 3.

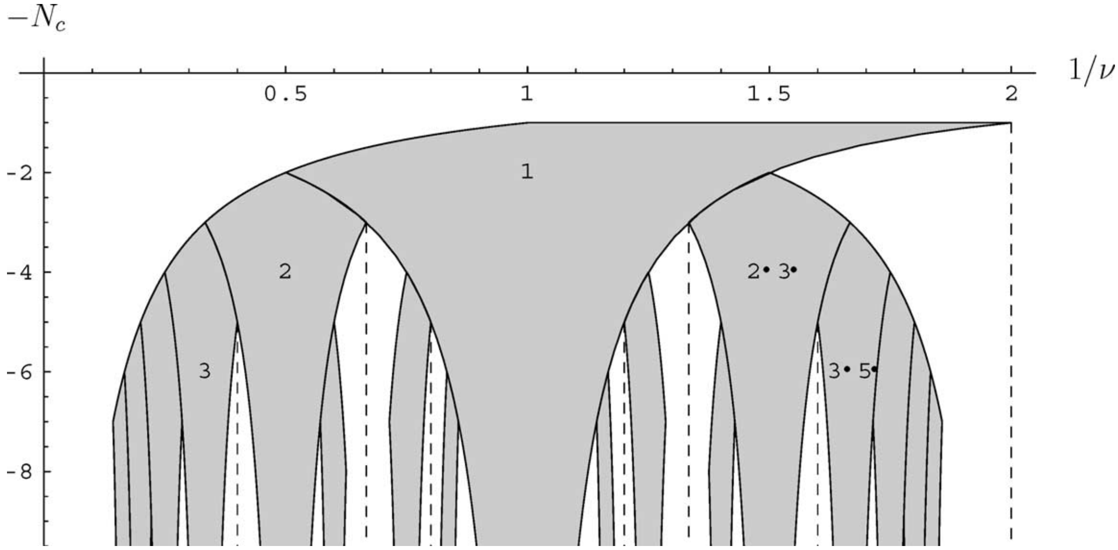

Fig. 5. Global phase diagram in the $(1/\nu,\ N_c)$ plane. Some phases are labelled by their corresponding values of ν. The Ins_H insulator phase (see text) (respectively, Ins_V) correspond to the uppermost outer region (respectively, to the leftmost region). The dashed lines represent some metallic states as in Fig. 4. Some possible insulator-liquid phases transitions are $\mathrm{Ins}_H \leftrightarrow 1$, $\mathrm{Ins}_H \leftrightarrow 1/3$, $\mathrm{Ins}_V \leftrightarrow 1$ and $\mathrm{Ins}_V \leftrightarrow 2$ (see also Fig. 6). Some possible liquid–liquid phases transitions are $1 \leftrightarrow 2$, $1 \leftrightarrow 2/3$ and $2 \leftrightarrow 3$.

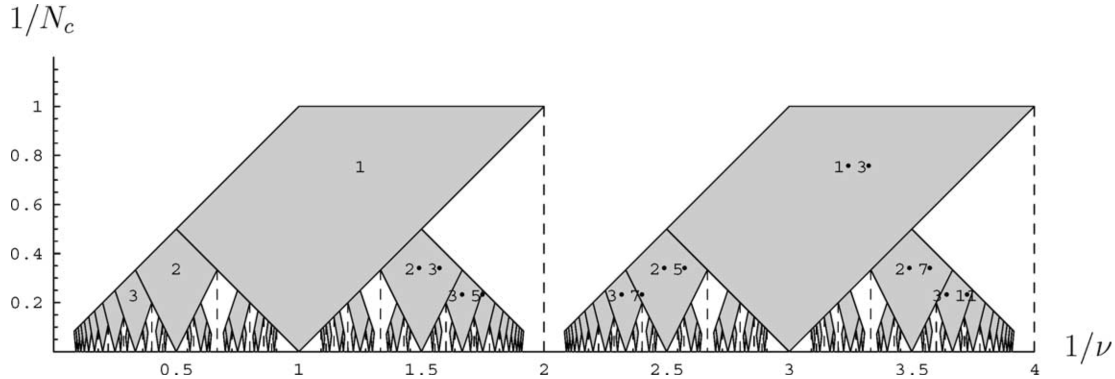

Fig. 6. Global phase diagram in the $(1/\nu,\ 1/N_c)$ plane. Owing to the choice of the $1/N_c$ variable, all the phases are represented by compact domains. More phases can be represented and the global topology of the diagram is more apparent.

the diagram obtained by superposing the odd–odd and odd–even visibility diagrams so that the conclusions of [10c] about the possible symmetry groups for the QHE are not altered.

One important remark is in order. One might choose other (more complicated) prescriptions to deal with the overlapping stripes which would therefore possibly modify the shape of some parts of the corresponding boundaries but would not alter definitely the global architecture of the phases, their relative positions, the whole topology of the phase diagram and the main predictions for the transitions stemming from that diagram. The prescription we have chosen is in fact consistent with the underlying assumption that the width of the cross over regions occurring between the various transitions at nonzero temperature, says $\Delta B(T)$, drops to zero when the temperature goes to zero. This is in fact reflected in the phase diagrams by the existence of common lines in the boundaries separating two phases thus allowing for a sharp transition between two adjacent plateaus. Although the possibility of having $\Delta B(T) \to 0$ at $T \to 0$ has been argued in earlier works based on scaling analysis and seems to be favored by some extrapolations stemming from experimental data [15], the situation concerning the possibility to have nonzero width for the cross over regions at zero temperature cannot be ruled out at the present time. A phenomenological way to take this last possibility into account in the construction of the phase diagram within the present framework would be to supplement the prescription described above by the additional assumption that common lines in the boundaries separating two adjacent plateaus are forbidden.

Up to now we have considered the quantum Hall liquid states associated with the odd denominator stripes. As far as the metallic states associated with even denominator stripes of Fig. 3 are concerned, a construction similar to the one presented in the previous section gives rise to the $\nu =$ odd/even stripes which can be superposed to the one for the quantum Hall liquid states without overlap. These stripes has not been represented on the phase diagrams Figs. 4 and 5, where only the directions of some of them are represented by dashed lines. They would fill in the empty regions around these dashed lines. In the rest of this Letter, we focalize mainly on the quantum Hall liquid states.

4. Discussion and conclusion

Summarizing the previous section, the present framework, if physically correct, predicts a zero temperature global phase diagram for the QHE depicted in Figs. 4 and 5. The physical relevance of this framework is supported at least by the successful comparison between some earlier predictions and experimental results as already reported in [10b,10c]. It seems to have captured some interesting features of the quantum Hall systems which are encoded in a rather simple symmetry principle based on the modular groups mentioned above linked with the visibility diagrams.

Let us now discuss the main features of the phase diagrams and confront them to the experimental and theoretical situation. The predicted phase diagram in the (B, N_c) plane (Fig. 4) involves a succession of stripes, each one corresponding to a quantum Hall liquid phase indexed by an integer or fractional filling factor, surrounded by two regions built from the lowermost white horizontal and leftmost vertical white region which must be interpreted physically. The former region corresponds to a quantum Hall phase indexed by $\nu = 0/1$. On Fig. 5, this phase corresponds to the uppermost outer region (close to the $1/\nu$ axis). According to the usual experimental analysis presented in, e.g., [12a], this would correspond to a strong disorder regime[4] in which basically the disorder potential dominates all other energies resulting in an insulating phase. The latter region, the vertical stripe, corresponds to a quantum Hall phase with $\nu =$“1/0” which, owing to (4), can be associated with a very weak applied magnetic field for which all states are expected to be localized and resulting again in an insulating phase. Notice that numerical studies focused on the integer QHE (mainly based on the TBM Hamiltonian) have suggested [16] the possible existence of two distinct insulating phases in the quantum Hall systems. Although the status of these insulating phases is not clear at the present time, we note furthermore that the phase diagram obtained in [16] is in good agreement with recent experimental results [12] to be discussed in a while.

As a first salient feature, the present framework predicts the existence of two insulating phases. These latter are denoted hereafter by Ins_H (respectively, Ins_V) corresponding to the horizontal (respectively, vertical) stripe of Fig. 4. The counterpart of Fig. 4 in the $(1/\nu,\ N_c)$ plane is shown on Fig. 5 where now the Ins_H (respectively, Ins_V) phase corresponds to the uppermost outer region (respectively, the leftmost region). As a remark, notice that there are some trajectories through the phase diagram which met only the integer quantum Hall liquid phases. This is indeed the case of any vertical straight line for B between 1 and 2 in our arbitrary units, as it can be seen on Fig. 4. These trajectories can be generated experimentally when one increases N_c by acting on the gate voltage while keeping fixed the magnetic field, which is actually the initial situation for the integer quantum Hall experiment.

[4] A relation involving the disorder and N_c is given for instance by the Drude model [14]. Here, we will not need any such exact relation.

One noticeable prediction concerning our global phase diagram is the possibility to have direct transitions from an insulting phase to any integer ν as well as $\nu = 1/(2k+1)$ ($k \in \mathbb{N}$) fractional quantum Hall liquid phases, as it can be easily realized from Figs. 4 and 5. Indeed, first observe that the $\nu = 1$ liquid phase is bordered by the Ins_H insulator so that the transition $\mathrm{Ins}_H \to 1$ is allowed. Now, the successive actions of Σ on that transition will give rise to all the allowed transitions of that type, namely

$$\mathrm{Ins}_H \to \frac{1}{2k+1}, \quad k \in \mathbb{N}. \tag{6}$$

Besides, the successive actions of products of different powers of T and Σ on $\mathrm{Ins}_H \to 1$ will generate all the other Ins_H–plateau and plateau–plateau transitions. Next, observe that any quantum Hall liquid phase with $\nu = 1/k$ ($k \in \mathbb{N}$) is bordered by the Ins_V insulating phase, so that any transition

$$\mathrm{Ins}_V \to k, \quad k \in \mathbb{N} \tag{7}$$

is allowed, according to the present framework. Of course, one easily observes that successive actions of T on the (template) transition $\mathrm{Ins}_V \to 1$ gives rise to the allowed transitions (7).

The possibility for having allowed direct insulating phase to quantum Hall liquid transitions appears to be a salient feature of the present construction. It appears that this last prediction contradicts the one proposed in [5] where the law of the corresponding states is also presented and discussed. To be more definite, consider the case of integer QHE. Then, in [5], the law of the corresponding states is combined with plausible (mainly) phenomenological arguments to propose a selection rule for the (integer) transitions. Namely, it is argued that the variation $\Delta\nu$ of the filling factor when one crosses the frontier separating two adjacent phases must satisfy

$$\Delta\nu = \pm 1 \tag{8}$$

shape including the insulator associated with $\nu = 0$. From this, one concludes that all the direct insulator–(integer) plateau transitions are forbidden except the $0 \to 1$ transition (therefore insulator $\to 1$ transition). In our framework, this rule cannot be applied to the $\nu =$"1/0" insulating phase (Ins_V). However, it remains valid for any finite value of ν, including the $\nu = 0$ case, that is, the insulator Ins_H. In the present framework, while the phase Ins_H can be considered as a quantum Hall liquid-like phase (with zero Hall conductivity), the Ins_V phase has a quite different origin. It is necessarily associated with the stripes of the even–odd diagram involving all the metallic states which are expected to have a behaviour different from the one of the quantum Hall liquid states.

An earlier theoretical phase diagram has been proposed in [17]. This diagram has some similarities with the one derived in [5] but predicts the occurrence of direct transitions from insulator to integer quantum Hall states. In some recent numerical studies [16], a phase diagram with allowed direct insulator to integer quantum Hall states transitions has been obtained whose topology is in good agreement with our phase diagrams.

As far as experimental results are concerned, we first note that in the present situation further studies are needed. In particular, the precise shape of the boundaries separating the various quantum Hall phases seems to be somehow dependent on the nature of the sample (and/or on possible spin effects). Nevertheless, the authors of [12a] have proposed a phase diagram obtained from an analysis of several direct transitions observed in Si MOSFETs. The transitions stemming from the topology of our phase diagram are in good agreement with the results reported in [12a].[5] In particular, direct transitions from insulator to (integer) quantum Hall liquid states are observed. A similar conclusion concerning those direct transitions has been reported in other experiments performed in Ge/SiGe systems and in p-type GaAs/AlGaAs devices [12b]. More recently, another experimental phase diagram for the integer QHE obtained from a two-dimensional hole system confined in a Ge/SiGe quantum well has been reported in [12c] in which again direct transitions from insulator to integer states were observed.

Let us discuss now some theoretical aspects connected to the modular subgroups introduced in the present work. The fact that the selection rule proposed in [5] seems to be experimentally violated does not rule out at the present time $\Gamma_0(2)$ as a possible candidate for a symmetry group relevant for the description

[5] Note however the possible occurrence of oscillations of the insulator to integer boundaries which are discussed in first of [12a].

of (some of) the global properties of the QHE. Recall that $\Gamma_0(2)$ is the modular symmetry underlying the law of the corresponding states of [5]. In fact, it can be easily realized that our phase diagram is consistent with the $\Gamma_0(2)$ symmetry with the selection rule (8) (integer case) enlarged to take into account the Ins_V state ($\nu = \infty$). Namely, the enlarged selection rule is

$$\begin{cases} \Delta\nu = \pm 1 & \text{for finite } \nu,\ \nu \in \mathbb{N}, \\ \mathrm{Ins}_V(\nu = \infty) \to 1 & \text{allowed.} \end{cases} \tag{9}$$

From this, the action of $\Gamma_0(2)$ generates all the allowed transitions of the phase diagram. We now have to examine the possible role of $\Gamma(2)$ in the present framework which may be viewed as a modification of the law of the corresponding states. Recall that the action of $\Gamma(2)$ on rational filling factors preserves the even or odd character of the numerators. Then, the theoretical analysis that gave rise to the enlarged selection rule for $\Gamma_0(2)$ can be easily adapted to $\Gamma(2)$ with the conclusion that consistency requires a further modification of the selection rule (9) given by

$$\begin{cases} \Delta\nu = \pm 1 & \text{for finite } \nu,\ \nu \in \mathbb{N}, \\ \mathrm{Ins}_V(\nu = \infty) \to 1 & \text{allowed,} \\ \mathrm{Ins}_V(\nu = \infty) \to 2 & \text{allowed.} \end{cases} \tag{10}$$

Although the predictions we obtain seems to agree with the present experimental, there is no argument within the present framework favoring $\Gamma(2)$ or $\Gamma_0(2)$ as being the most suitable candidate as a symmetry group relevant for the QHE. Notice however that some works suggest that it may be physically relevant to distinguish even from odd numerator filling fractions [13]. At this point, let us go back to the discussion presented at the end of Section 2.2. It is known that the importance of the spin degrees of freedom depends basically of the (effective) g-Landé factor of the charge carriers determining the magnitude of the Zeeman energy E_z relative to the cyclotron energy E_c at a given filling factor. For the GaAs devices as in first of [12b], the Zeeman to cyclotron energy ratio E_z/E_c is small. Typical values are $E_c \sim 20B$ and $E_z \sim 0.3\,B$ (B in Tesla and energies in Kelvin). Then, according to the discussion presented at the end of Section 2.2, the splitted Landau levels come to be organized into well separated pairs, each level being close to each other within each pair so that T^2 seems to be more suitable to describe the Landau level addition operator (which therefore may favor $\Gamma(2)$). A Zeeman to cyclotron energy ratio very close to 0.5 would result in evenly separated levels so that obviously the Landau level addition would be more appropriately described by T. In the experiment [12c], the Zeeman to cyclotron energy ratio $E_z/E_c \sim 0.7$ (not to far away from 0.5) producing relatively well separated Landau levels. For this value, it is easy to realize that the resulting splitted levels are organized into pairs with spacing between the levels of each pair $\Delta E/E_c \sim 0.4$ whereas the spacing between a given level of a pair and the corresponding level involved in the upper pair is equal to the cyclotron energy. In that latter situation, a more quantitative analysis beyond the comparison of some orders of magnitude is needed to obtain some reliable indication possibly favoring one out of the two considered modular subgroups.

In conclusion, we have constructed from the visibility diagrams encoding some rather simple symmetry principle based on modular subgroups [10] a zero temperature global phase diagram for the QHE depicted in Figs. 4 and 5. From this phase diagram, we predict the existence of two insulating phases. One other noticeable prediction is the possibility to have direct transitions from an insulting phase to any integer as well as $\nu = 1/(2k+1)$ ($k \in \mathbb{N}$) fractional quantum Hall liquid phases which seems to agree with some recent experimental observations. We also propose selection rules for the possible plateau–plateau (and plateau–insulators) transitions which may constitute testable predictions.

References

[1] K.V. Klitzing, G. Dorda, M. Pepper, Phys. Rev. Lett. 45 (1980) 494;
D.C. Tsui, H.L. Störmer, A.C. Gossard, Phys. Rev. Lett. 48 (1982) 1559.
[2] For a review, see, in: R.E. Prange, S.M. Girvin (Eds.), The Quantum Hall Effect, 2nd edn., Springer, New York, 1990;
See also, in: S.D. Sarma, A. Pinczuk (Eds.), Perspectives in Quantum Hall Effect, Wiley, New York, 1997;
M. Stone, The Quantum Hall Effect, World Scientific, Singapore, 1992.
[3] S.M. Girvin, A.H. MacDonald, Phys Rev. Lett. 58 (1987) 1252;
See also: S.M. Girvin, in: R.E. Prange, S.M. Girvin (Eds.), The Quantum Hall Effect, 2nd edn., Springer, New York, 1990, Chapter 10.
[4] S.C. Zhang, T.H. Hanson, S. Kivelson, Phys. Rev. Lett. 62 (1989) 82;

See for a review: S.-C. Zhang, Int. J. Mod. Phys. B 6 (1992) 25.
[5] S. Kivelson, D.H. Lee, S.-C. Zhang, Phys. Rev. B 46 (1992) 2223.
[6] Some mathematical background for modular group can be found in: R.A. Rankin, Modular Forms and Functions, Cambridge Univ. Press, 1997.
[7] C.A. Lütken, G.G. Ross, Phys. Rev. B 45 (1992) 11837;
C.A. Lütken, G.G. Ross, Phys. Rev. B 48 (1993) 2500;
A. Shapere, F. Wilczek, Nucl. Phys. B 320 (1989) 669;
C.A. Lütken, Nucl. Phys. B 396 (1993) 670.
[8] For a detailled analysis, see: C.P. Burgess, B.P. Dolan, Phys. Rev. B 63 (2001) 155309.
[9] B.P. Dolan, J. Phys. A 32 (1999) L243;
B.P. Dolan, Nucl. Phys. B 554 (1999) 487;
B.P. Dolan, Phys. Rev. B 62 (2000) 10278;
See also: C.P. Burgess, B.P. Dolan, Phys. Rev. B 63 (2001) 155309.
[10] (a) Y. Georgelin, J.-C. Wallet, Phys. Lett. A 224 (1997) 303;
Y. Georgelin, T. Masson, J.-C. Wallet, J. Phys. A 33 (2000) 39;
(b) Y. Georgelin, T. Masson, J.-C. Wallet, J. Phys. A 30 (1997) 5065;
(c) Y. Georgelin, T. Masson, J.-C. Wallet, J. Phys. A 33 (2000) 8649.
[11] D.H. Cobden, C.H. Barnes, C.J.B. Ford, Phys. Rev. Lett. 82 (1999) 4695.
[12] (a) S.V. Kravchenko, W. Mason, J.E. Furneaux, V.M. Pudalov, Phys. Rev. Lett. 75 (1995) 910;
S.V. Kravchenko, G.V. Kravchenko, J.E. Furneaux, V.M. Pudalov, M. D'Iorio, Phys. Rev. B 50 (1994) 8039;
(b) S.H. Song, D. Shahar, D.C. Tsui, Y.H. Xie, D. Monroe, Phys. Rev. Lett. 78 (1997) 2200;
S.C. Dultz, H.W. Jiang, W.J. Schaff, Phys. Rev. B 58 (1998) R7532;
(c) M. Hilke, D. Shahar, S.H. Song, D.C. Tsui, Y.H. Xie, Phys. Rev. B 62 (2000) 6940.
[13] See A.M. Chang, in: R.E. Prange, S.M. Girvin (Eds.), The Quantum Hall Effect, 2nd edn., Springer, New York, 1990;
H.E. Cage, in: R.E. Prange, S.M. Girvin (Eds.), The Quantum Hall Effect, 2nd edn., Springer, New York, 1990;
See also L.P. Levy, et al., Magnetization oscillations at fractional filling factors, in: ITP Conference on Disorder and Interactions in Quantum Hall and Mesoscopic Systems, 1998.
[14] For a discussion, see A. Karlhede, S.A. Kivelson, S.L. Sondhi, in: V.J. Emery (Ed.), Correlated Electron Systems, World Scientific, Singapore, 1993.
[15] See R.E. Prange, in: R.E. Prange, S.M. Girvin (Eds.), The Quantum Hall Effect, 2nd edn., Springer, New York, 1990;
For more details see Y.S. Wu, in: H.C. Lee (Ed.), Lecture Notes given at NATO Advanced Summer Institute "Physics, Geometry and Topology" at Banff, Canada, Plenum, 1989.
[16] D.N. Sheng, Z.Y. Weng, cond-mat/9906261;
D.N. Sheng, Z.Y. Weng, X.G. Wen, Phys. Rev. B 64 (2001) 165317.
[17] B.J. Halperin, P.A. Lee, N. Read, Phys. Rev. B 47 (1993) 7312.